Int. J. Solids Structures Vol. 18, No. 8, pp. 659–672, 1982
Printed in Great Britain.

0020-7683/82/080659-14$03.00/0

MATERIAL FAILURE BY VOID COALESCENCE IN LOCALIZED SHEAR BANDS

VIGGO TVERGAARD
Department of Solid Mechanics, The Technical University of Denmark, Lyngby, Denmark

(*Received* 25 *August* 1981; *in revised form* 16 *December* 1981)

Abstract—For a void containing ductile material a continuum model of the loss of stress carrying capacity due to void coalescence is suggested. This model is included in a set of constitutive reactions for a ductile porous material, such that the process of void coalescence is assumed active, when the local void volume fraction has exceeded a critical value. Predictions of the model are illustrated by a number of simple analyses of shear band development in uniformly strained solids. Furthermore, the failure model is applied in a numerical analysis of strain localization and fracture by a void sheet mechanism in the matrix material between two larger voids. When coalescence has taken place in a small material region, this part of the material has no more stress-carrying capacity. In the continued computations such totally failed material is described as a fictitious elastic-plastic material with a very low yield stress.

1. INTRODUCTION

In a ductile metals failure by coalescence of microscopic voids is an important fracture mechanism. Voids nucleate mainly at second phase particles, by particle fracture or by interfacial decohesion, and subsequently the voids grow due to plastic straining of the surrounding material. Fracture by coalescence occurs when the ligaments between neighbouring voids have thinned down sufficiently. Such general coalescence is often observed in the centre of the neck in a round tensile bar. In other cases localization of plastic flow takes place, so that the void induced failure occurs inside a narrow shear band by the formation of a void sheet.

Approximate estimates of the critical strain for coalescence can be obtained on the basis of analyses of the growth of a single void in an infinite block of plastic material[1–3], or by computations for periodic arrays of voids[4]. In the continuum description of a porous ductile material suggested by Gurson[5, 6] the effect of void coalescence is not directly accounted for; but the load carrying capacity of the material vanishes as the void volume fraction approaches unity.

Experimental studies discussed by Brown and Embury[7] and Goods and Brown[8] indicate that coalescence occurs approximately when the length of the voids is equal to their spacing. This means that the volume fraction of voids at fracture is far below unity, in the range of say 0.1–0.2. Based on these results it seems reasonable to use a critical value of the void volume fraction as a criterion of final material failure in computations employing Gurson's model. This is particularly useful in cases where the failure criterion is satisfied simultaneously all over a narrow region separating to body in two, as in the cases studied by Chu and Needleman[9]. However, in many cases failure will propagate into the material, see for example Tvergaard[10], and here a more detailed description of the local loss of load carrying capacity at failure is required.

A material model that approximately describes the nucleation, growth and finally coalescence of voids could be obtained by fitting experimental data with the parameters in a set of rather general constitutive relations accounting for plastic dilatancy and for the possibility of non-normality. Such constitutive relations have been suggested by Rudnicki and Rice[11] with the main intention of describing the behaviour of rocks or soils. The same type of relations have been discussed by Mróz[12], and an alternative formulation is given recently by Nemat-Nasser and Shokooh[13]. The porous material model of Gurson[5] does in fact belong to the class of materials treated in [11], see Needleman and Rice[14]. This model limits the freedom of choice of material parameters, by requiring agreement with simple rigid-plastic void growth analyses; but still a number of parameters are free to be fitted with experimental data.

In the present paper the macroscopic effect of void coalescence is modelled within the context of the Gurson model. The ductile fracture process is described as an apparent loss of

active material volume, with a corresponding rapid decay of the average macroscopic stresses. To illustrate the model the development of ductile fracture in shear bands is studied for a variety of stress-states, assuming a homogeneous state of deformation inside and outside the band, respectively. Furthermore, the model of coalescence is introduced in a numerical study of a ductile fracture mechanism involving the interaction of larger voids with relatively small voids[10]. In this computation the porous ductile material model is used to describe the nucleation, growth and coalescence of small scale voids in the matrix material surrounding the larger voids.

2. MATERIAL FAILURE MODEL

The possibility of final material failure, at some critical void volume fraction considerably below unity, shall here be modelled within the context of the constitutive relations suggested by Gurson[5, 6]. These relations make use of an approximate yield condition, of the form $\Phi(\sigma^{ij}, \sigma_M, f) = 0$, for a void containing ductile material. Here σ^{ij} is the average macroscopic Cauchy stress tensor, σ_M is an equivalent tensile flow stress representing the actual microscopic stress-state in the matrix material, and f is the current void volume fraction.

Based on a number of experimental studies Brown and Embury[7] find that after nucleation cavities elongate along the major tensile axis, and that two neighbouring cavities coalesce when their length has grown to the order of magnitude of their spacing. This local failure occurs by the development of slip planes between the cavities or simply necking of the ligament. The critical void volume fraction estimated in [7] by a simple model is $f_C \simeq 0.15$; but certainly, depending on differences of microstructures, stress-states, etc. this value could vary in a range of say 0.1–0.2.

When necking of the ligaments starts to occur, the stress carrying part of the cross-section decreases much faster with further straining than predicted by a model assuming spherical or circular cylindrical voids evenly distributed in the material. As a consequence the average macroscopic stresses σ^{ij} decay rapidly. Such effects could be accounted for in the construction of the yield function Φ; but it seems natural, instead, to model this failure process as a loss of active material volume, locally.

The change of the void volume fraction during an increment of deformation is usually taken to be the sum of a contribution from the growth of existing voids and a contribution from the nucleation of new voids. Here, an extra contribution modelling the failure process shall be added, when the current void volume fraction exceeds a critical value. Thus, with $\dot{(\ )}$ denoting differentiation with respect to a loading parameter, we take

$$\dot{f} = (\dot{f})_{\text{growth}} + (\dot{f})_{\text{nucleation}} + (\dot{f})_{\text{failure}}. \tag{2.1}$$

Before giving expressions for the different terms in (2.1) a few definitions corresponding to a Lagrangian formulation of the field equations shall be introduced. A material point is identified by the coordinates x^i in the reference configuration, and the displacement components relative to this reference coordinate system are u^i. The increment of the Lagrangian strain tensor η_{ij} is given by

$$\dot{\eta}_{ij} = \frac{1}{2}(\dot{u}_{i,j} + \dot{u}_{j,i} + \dot{u}^k_{,i}u_{k,j} + u^k_{,i}\dot{u}_{k,j}) \tag{2.2}$$

where $()_{,i}$ denotes covariant differentiation in the reference configuration. The contravariant components of the Cauchy stress tensor σ^{ij} and of the Kirchhoff stress tensor τ^{ij}, on the embedded deformed coordinates, are related by the expression

$$\tau^{ij} = \sqrt{(G/g)}\,\sigma^{ij} \tag{2.3}$$

where G and g are the determinants of the metric tensors G_{ij} and g_{ij} in the current configuration and in the reference configuration, respectively. Indices range from 1 to 3, and the summation convention is adopted for repeated indices.

The matrix material is taken to be plastically incompressible. Thus, the increment in (2.1) due to the growth of existing voids is given by

$$(\dot{f})_{\text{growth}} = (1-f)G^{ij}\dot{\eta}_{ij}^{P} \tag{2.4}$$

where $\dot{\eta}_{ij}^{P}$ is the plastic part of the macroscopic strain increment. Nucleation of new voids occurs mainly at second phase particles, by decohesion of the particle-matrix interphase or by particle fracture. Needleman and Rice[14] have suggested a nucleation model of the form

$$(\dot{f})_{\text{nucleation}} = \mathscr{A}\dot{\sigma}_M + \mathscr{B}(\dot{\sigma}_k^k)/3 \tag{2.5}$$

which shall be used here. More complex nucleation models have been discussed by Gurson[6].

The effective plastic strain ϵ_M^P, representing the microscopic strain-state in the matrix material, is related to σ_M by the incremental equation

$$\dot{\epsilon}_M^P = \left(\frac{1}{E_t} - \frac{1}{E}\right)\dot{\sigma}_M \tag{2.6}$$

where E is Young's modulus, and E_t is the slope of the uniaxial true stress-natural strain curve for the matrix material at the current stress level σ_M. Thus, a material, for which void nucleation is controlled by the plastic strain [8], can be modelled in terms of (2.5), by taking $\mathscr{A} > 0$ and $\mathscr{B} = 0$. For materials, in which nucleation is controlled by the maximum normal stress on the particle-matrix interphase, Needleman and Rice[14] have suggested using the sum $\sigma_M + \sigma_k^k/3$ as an approximate measure of this maximum stress, thus taking $\mathscr{A} = \mathscr{B}$ in (2.5).

The final material failure, by local necking of the ligaments, is a process that develops mainly as a function of material straining. Here, ϵ_M^P shall be used as a measure of this straining. Thus, the last term in (2.1) is modeled by an expression of the form

$$(\dot{f})_{\text{failure}} = \mathscr{C}\dot{\sigma}_M \tag{2.7}$$

which is analogous with the first term on the right hand side of (2.5). As long as the void volume fraction f is smaller than a critical value f_C, $\mathscr{C} = 0$ is used in (2.7). However, for larger f the void volume fraction is taken to increase linearly with ϵ_M^P, so that total failure occurs after an additional straining of magnitude $\Delta\epsilon$. Thus, using (2.6), the following expression is obtained

$$\mathscr{C} = \left(\frac{1}{E_t} - \frac{1}{E}\right)\frac{f_U - f_C}{\Delta\epsilon}, \text{ for } f \geq f_C. \tag{2.8}$$

Here, f_U is the ultimate value of the void volume fraction, at which no further macroscopic stresses can be carried by the material.

The increment of the void volume fraction, $(\dot{f})_{\text{failure}}$, used here to simulate the effect of final material failure could be assumed to depend on $\dot{\epsilon}_M^P$ in a more complex manner than that suggested by (2.8). However, the linear dependence is considered sufficient for the present investigation.

The parameters $\mathscr{A}$ and $\mathscr{B}$ in (2.5) are chosen so that void nucleation follows a normal distribution [9]. Thus, for a material with plastic strain controlled nucleation we shall use

$$\mathscr{A} = \left(\frac{1}{E_t} - \frac{1}{E}\right)\frac{f_N}{s\sqrt{(2\pi)}}\, e^{-1/2\{(\epsilon_M^P - \epsilon_N)/s\}^2}, \quad \mathscr{B} = 0 \tag{2.9}$$

where f_N is the volume fraction of void nucleating particles, ϵ_N is the mean strain for nucleation, and s is the corresponding standard deviation. For a material with stress controlled nucleation the similar expressions are

$$\mathscr{A} = \mathscr{B} = \frac{f_N}{s\sqrt{(2\pi)}}\, e^{-1/2\{((\sigma_M + \sigma_k^k/3) - \sigma_N)/s\}^2} \tag{2.10}$$

where σ_N is the mean nucleation stress.

The nonzero values of $\mathscr{C}$ and $\mathscr{A}$ specified by (2.8) and (2.9) are only used, if ϵ_M^P exceeds its current maximum in the increment considered. Also, for stress controlled nucleation $\mathscr{A} = \mathscr{B} = 0$ is used instead of (2.10), if the value of $\sigma_M + \sigma_k^k/3$ is not going to exceed the maximum value reached in the previous stress history.

3. CONSTITUTIVE RELATIONS

The approximate yield condition derived by Gurson[5], based on a rigid-perfectly plastic upper bound solution for spherically symmetric deformations around a single spherical void, is of the form

$$\Phi = \frac{\sigma_e^2}{\sigma_M^2} + 2fq_1 \cosh\left\{\frac{q_2}{2}\frac{\sigma_k^k}{\sigma_M}\right\} - (1 + q_3 f^2) = 0 \tag{3.1}$$

for $q_1 = q_2 = q_3 = 1$. Here, $\sigma_e = (3s_{ij}s^{ij}/2)^{1/2}$ is the macroscopic effective Mises stress, and $s^{ij} = \sigma^{ij} - G^{ij}\sigma_k^k/3$ is the stress deviator.

The effective plastic strain ϵ_M^P in the matrix material is assumed to vary according to the equivalent plastic work expression

$$\sigma^{ij}\dot{\eta}_{ij}^P = (1-f)\sigma_M\dot{\epsilon}_M^P. \tag{3.2}$$

Thus, using (2.6), the following expression is found for the increment of the equivalent tensile flow stress

$$\dot{\sigma}_M = \frac{EE_t}{E - E_t}\frac{\sigma^{ij}\dot{\eta}_{ij}^P}{(1-f)\sigma_M}. \tag{3.3}$$

The plastic part of the macroscopic strain rate is taken to be given by

$$\dot{\eta}_{ij}^P = \Lambda\frac{\partial\Phi}{\partial\sigma^{ij}} \tag{3.4}$$

since normality for the matrix material implies macroscopic normality[15]. The value of the parameter Λ is determined from the consistency condition $\dot{\Phi} = 0$, required during plastic loading. Substituting (3.3), (2.1), (2.5) and (2.7) into this condition gives

$$\dot{\eta}_{ij}^P = \frac{1}{H}\left[\frac{3}{2}\frac{s_{ij}}{\sigma_M} + \alpha G_{ij}\right]\left[\frac{3}{2}\frac{s_{kl}}{\sigma_M} + \beta G_{kl}\right]\overset{\nabla}{\sigma}{}^{kl} \tag{3.5}$$

where $\overset{\nabla}{\sigma}{}^{kl}$ is the Jaumann rate of the Cauchy stress tensor

$$\overset{\nabla}{\sigma}{}^{kl} = \dot{\sigma}^{kl} + (G^{km}\sigma^{ln} + G^{lm}\sigma^{kn})\dot{\eta}_{mn} \tag{3.6}$$

and the parameters α, β and H are given by

$$\alpha = \frac{f}{2}q_1q_2\sinh\left\{\frac{q_2}{2}\frac{\sigma_k^k}{\sigma_M}\right\},\ \beta = \alpha + \frac{\mathscr{B}\sigma_M}{6}\frac{\partial\Phi}{\partial f} \tag{3.7}$$

$$H = \frac{\sigma_M}{2}\left[-3\alpha(1-f)\frac{\partial\Phi}{\partial f} - \left\{\frac{\partial\Phi}{\partial f}(\mathscr{A} + \mathscr{C}) + \frac{\partial\Phi}{\partial\sigma_M}\right\}\frac{EE_t}{E - E_t}\frac{1}{1-f}\left(\frac{\sigma_e^2}{\sigma_M^2} + \alpha\frac{\sigma_k^k}{\sigma_M}\right)\right]. \tag{3.8}$$

During plastic loading, with $\Phi = 0$, the condition for continued plastic deformation is $\Lambda \geq 0$ in (3.4)

$$\frac{1}{H}\left[\frac{3}{2}\frac{s_{kl}}{\sigma_M} + \beta G_{kl}\right]\overset{\nabla}{\sigma}{}^{kl} \geq 0. \tag{3.9}$$

Thus, the yield surface differs from $\Phi = 0$, unless $\beta = \alpha$ ($\mathscr{B} = 0$). The function Φ is still used as a plastic potential, though.

When $\Phi = 0$ is reached during elastic deformation, the condition for plastic loading is that $\dot{\Phi} > 0$ would result, if elastic deformation continued

$$\left[\frac{3}{2}\frac{s_{kl}}{\sigma_M} + \beta G_{kl}\right]\overset{\nabla}{\sigma}{}^{kl} > 0. \tag{3.10}$$

When the macroscopic hardening rate H is negative, (3.10) differs from (3.9).

The total strain rate $\dot{\eta}_{ij}$ is taken to be the sum of the plastic part $\dot{\eta}_{ij}^{P}$ and the elastic part

$$\dot{\eta}_{ij}^{E} = \frac{1}{E}\{(1+\nu)G_{ik}G_{jl} - \nu G_{ij}G_{kl}\}\overset{\nabla}{\sigma}{}^{kl}. \tag{3.11}$$

The inverse of this sum is an expression of the form $\overset{\nabla}{\sigma}{}^{ij} = R^{ijkl}\dot{\eta}_{kl}$, which is transformed into the incremental constitutive relations

$$\dot{\tau}^{ij} = L^{ijkl}\dot{\eta}_{kl} \tag{3.12}$$

using (3.6) and the incremental form of (2.3). Detailed expressions for the instantaneous moduli L^{ijkl} are given in [10] and shall not be repeated here; but it should be emphasized that in general $L^{ijkl} \neq L^{klij}$ for the present model.

The ultimate value f_U of the void volume fraction, at which the macroscopic stress carrying capacity vanishes, is a property of the assumed yield function. Thus, for $\sigma_e = \sigma_k{}^k = 0$ eqn (3.1) gives

$$2f_U q_1 - 1 - q_3 f_U{}^2 = 0. \tag{3.13}$$

In the function suggested by Gurson, $q_1 = q_2 = q_3 = 1$, the ultimate void volume fraction is $f_U = 1$. This is due to the optimal material distribution implied by the spherically symmetric model problem, in which average macroscopic stresses can be carried as long as the volume of the central hole is smaller than that of the whole sphere.

Numerical studies of materials with periodically distributed circular cylindrical voids or spherical voids have been compared with predictions of the continuum model [16, 17], and it has been found that the agreement is considerably improved, if the yield condition suggested by Gurson is modified by using the set of parameters $q_1 = 1.5$, $q_2 = 1$ and $q_3 = q_1{}^2$ in (3.1). For $q_3 = q_1{}^2$ eqn (3.13) gives the ultimate void volume fraction $f_U = 1/q_1$, and thus the value corresponding to $q_1 = 1.5$ is $f_U = 2/3$. It may be noted that, even though the choice of the parameter value $q_1 = 1.5$ is based on computations for low void volume fractions, a value of f_U below unity is realistic. For example, the volume fraction of an array of "closely packed" spherical voids is well below unity. Yield functions of the form (3.1), for $q_3 = q_1{}^2$ and various values of f are shown in Fig. 1.

When the void volume fraction reaches the value f_U in a material point, no more average macroscopic stresses can be carried in that point (see Fig. 1), and the material separates

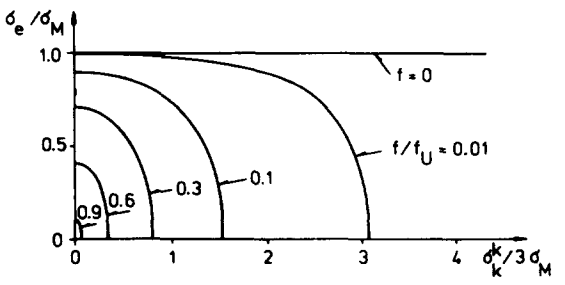

Fig. 1. Yield surface dependence on the hydrostatic tension for various values of the void volume fraction, when $q_2 = 1$ and $q_3 = q_1^2$ in (3.1).

completely. In a numerical computation this means that the boundary conditions should be changed continuously, as a region characterized by $f = f_{,/}$ grows, and a free boundary develops.

In the present paper an alternative approximate approach shall be tried, which is easily implemented in numerical computations. The material model described above is only used until the void volume fraction reaches a value f_U^*, slightly smaller than f_U. Subsequently, the "totally fractured" material is described by an elastic-plastic constitutive law appearing from eqns (3.1)–(3.12) by enforcing a constant void volume fraction $f = f_U^*$. The only changes necessary in doing so is replacing (2.1) by $\dot{f} = 0$ and prescribing $\partial\Phi/\partial f = 0$ in (3.7) and (3.8). Furthermore, the tangent modulus is given a small negative value, $E_t = \sigma_y - \sigma_M$, to ensure that σ_M does not increase. Here σ_y is the initial yield stress.

The approximate yield function used to describe the totally fractured material, for $f = f_U^*$, ensures that σ^{ij}/σ_M remain small (see Fig. 1). However, as large inelastic strains develop in the fractured region, these small stresses give rise to an energy dissipation not present in reality. The approximation is better the closer to unity f_U^*/f_U is chosen.

The need to take into account that $f = f_U$ may be reached in the material is not only related to the use of a failure model such as (2.7). Even in the absence of (2.7) the critical volume fraction will be reached, ultimately, although at somewhat higher strains.

The expression (3.11) assumed for the elastic part of the strain rate is only a good approximation as long as $f \ll 1$. However, the error due to neglecting voids in this expression in strongly damaged material regions is expected to be small, since the elastic contribution to the straining remains small throughout the deformation history.

4. SHEAR BAND DEVELOPMENT IN UNIFORMLY STRAINED SOLIDS

If an initial material inhomogeneity is assumed inside a thin, plane slice of material and the stress-states inside and outside this slice of material, respectively, as assumed to remain homogeneous throughout the deformation history, a relatively simple model problem for the study of shear band development is obtained. This model has been used by Yamamoto [18] to study the influence of an inhomogeneous void volume fraction distribution, based on Gurson's constitutive law, and Saje *et al.*[19] have included the influence of void nucleation.

Using the initial state as reference and a Cartesian reference coordinate system, the principal directions outside the band are taken to remain fixed, parallel with the x^i-axes. The major principal stress outside the band is taken to be in the x^1-direction (Fig. 2). The slice of material containing the initial inhomogeneity is assumed parallel withthe x^3-axis, with the initial angle of inclination ψ_I and the unit normal vector n_i.

Compatibility requires no jump in tangential derivatives of the displacements u_i over the band interphase. Thus

$$u^b_{\alpha,\beta} = u^0_{\alpha,\beta} + c_\alpha n_\beta, \quad u^b_{3,3} = u^0_{3,3} \tag{4.1}$$

where $()^b$ and $()^0$ denote quantities inside and outside the band, respectively, c_α are parameters to be determined, an Greek indices range from 1 to 2.

Equilibrium requires continuity of nominal tractions T^i over the band interphase

$$(T^\alpha)^b = (T^\alpha)^0 \tag{4.2}$$

where the tractions on a surface with reference normal n_j are given by

$$T^i = (\tau^{ij} + \tau^{ik}u^i_{,k})n_j. \tag{4.3}$$

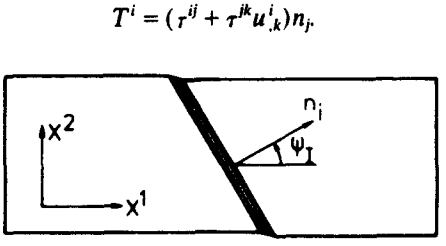

Fig. 2. Specimen in which a thin slice of material contains an initial inhomogeneity.

Now, substituting the incremental form of (4.3) into the incremental form of (4.2), using (2.2), (3.12) and (4.1), gives two incremental equations for $\dot{c}_\alpha$, provided that the stress or strain state outside the band is prescribed.

In the cases to be considered here the the state outside the band is taken to be characterized by the following fixed ratios of principal logarithmic strains ϵ_i and principal true stresses σ_i

$$\epsilon_3^0 = \gamma\epsilon_2^0, \quad \sigma_2^0 = \kappa\sigma_1^0 \tag{4.4}$$

where γ and κ are constants. The uniaxial true stress-logarithmic strain curve is taken to be represented by the piecewise power law

$$\epsilon = \begin{cases} \dfrac{\sigma}{E}, & \text{for } \sigma \le \sigma_y \\ \dfrac{\sigma_y}{E}\left(\dfrac{\sigma}{\sigma_y}\right)^n, & \text{for } \sigma > \sigma_y \end{cases} \tag{4.5}$$

where σ_y is the uniaxial yield stress, and n is the strain hardening exponent. Thus, for given values of the initial void volume fraction f_I and the nucleation and failure parameters, inside and outside the band, respectively, the solution is obtained incrementally.

The failure criterion usually applied, both for void containing materials [18, 19] and for other material descriptions [20], is strain rate reversal (elastic unloading) outside the band. Subsequent to this event high straining occurs inside the narrow band without contributing much to the overall straining of the body. However, in the present investigation, where modelling final material failure is of primary interest, the computations shall be continued beyond the point of elastic unloading.

Computations are carried out for a material with the initial yield stress specified by $\sigma_y/E = 0.0033$, Poisson's ratio $\nu = 0.3$ and the strain hardening exponent $n = 10$. Void nucleation is taken to be plastic strain controlled, according to (2.9), with $f_N = 0.04$, $\epsilon_N = 0.3$ and $s = 0.1$.

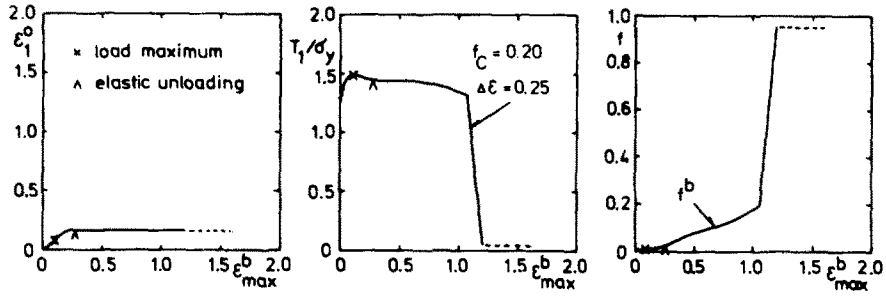

Fig. 3. Strain outside band ϵ_1^0, nominal traction T_1, and void volume fraction f, versus maximum principal logarithmic strain ϵ^b_{max} inside band; for $\epsilon_3^0 = 0$, $\sigma_2^0 = 0$, $\psi_I = 32.0°$, $f_I^b = 0.01$, $q_1 = 1$ and $f_I^b/f_U = 0.95$.

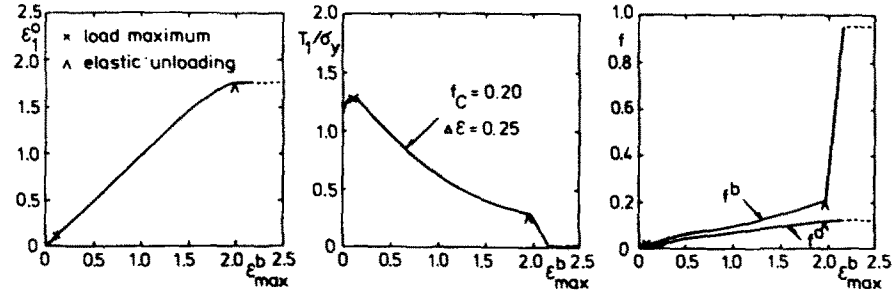

Fig. 4. Strain outside band ϵ_1^0, nominal traction T_1, and void volume fraction f, versus maximum principal logarithmic strain ϵ^b_{max} inside band; for $\epsilon_3^0 = \epsilon_2^0$, $\sigma_2^0 = \sigma_3^0 = 0$, $\psi_I = 3.5°$, $f_I^b = 0.01$, $q_1 = 1$ and $f_I^b/f_U = 0.95$.

The initial void volume fraction inside the band is taken to be $f_I^b = 0.01$, whereas outside the band $f_I^0 = 0$. In all cases $q_2 = 1$ and $q_3 = q_1^2$ is used for the yield function (3.1).

The parameter value $q_1 = 1$, and thus $f_U = 1$, is employed in Figs. 3 and 4 for uniaxial plane strain tension ($\gamma = \kappa = 0$) and for uniaxial tension ($\gamma = 1$, $\kappa = 0$), respectively. Furthermore, $f_C = 0.2$ and $\Delta\epsilon = 0.25$ are used in the material failure model (2.8) and at final failure $f_U^* = 0.95$ is assumed. The initial band inclinations in the two cases are taken to be $\psi_I = 32.0°$ and $\psi_I = 3.5°$, respectively, and the strains at which elastic unloading occurs outside the band agree with those found by Saje, Pan and Needleman[19] for the same initial angles. It should be noted that Saje *et al.*[19] have also determined the critical values of ψ_I, for which localization occurs at the smallest possible strain, whereas here one particular angle is chosen, slightly below the critical value.

Figures 3 and 4 show plots of the principal logarithmic strain ϵ_1^0, the nominal traction T_1, and the current void volume fraction f, versus the maximum principal logarithmic strain ϵ_{max}^b inside the band. In Fig. 3 the void volume fraction at elastic unloading is only around 0.04 inside the band, so that considerable further straining is required, before the process of final material failure starts according to (2.7) and (2.8). In Fig. 4 elastic unloading outside the band occurs at a larger void volume fraction, $f^b \simeq 0.20$, and in this case also the void volume fraction outside the band grows to a noticeable level. As soon as the critical volume fraction f_C is reached, so that the failure model (2.7) is active inside the band, the load carrying capacity decays rapidly towards zero and f^b approaches unity. Clearly, the cut-off at the volume fraction f_U^* slightly smaller than f_U is not realistic. However, it is noticed that with this artificial cut-off the computation continues beyond the point at which some material is totally fractured, without changes of the boundary conditions.

If Figs. 5 and 6 the computations of the two previous figures are repeated for the parameter value $q_1 = 1.5$ in the yield condition (3.1), and thus $f_U = 2/3$. This results in smaller strains ϵ_1^0 outside the band at localization, as expected[16, 17]. It is seen that also here the nominal tractions vanish, as the void volume fraction approaches the ultimate value f_U.

In the plane strain case, Fig. 5, computations for two additional sets of parameters, $f_C = 0.15$ and $\Delta\epsilon = 0.4$ or 0.6 in the failure model (2.8), are included too. The values of the strain ϵ_{max}^b at

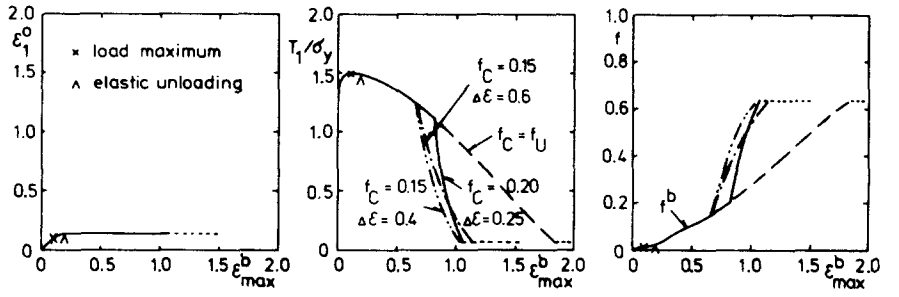

Fig. 5. Strain outside band ϵ_1^0, nominal traction T_1, and void volume fraction f, versus maximum principal logarithmic strain ϵ_{max}^b inside band; for $\epsilon_3^0 = 0$, $\sigma_2^0 = 0$, $\psi_I = 32.0°$, $f_I^b = 0.01$, $q_1 = 1.5$ and $f_U^*/f_U = 0.95$.

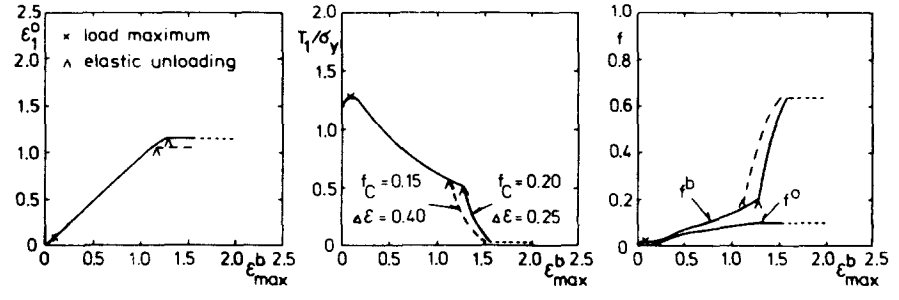

Fig. 6. Strain outside band ϵ_1^0, nominal traction T_1, and void volume fraction f, versus maximum principal logarithmic strain ϵ_{max}^b inside band; for $\epsilon_3^0 = \epsilon_2^0$, $\sigma_3^0 = \sigma_2^0 = 0$, $\psi_I = 3.5°$, $f_I^b = 0.01$, $q_1 = 1.5$ and $f_U^*/f_U = 0.95$.

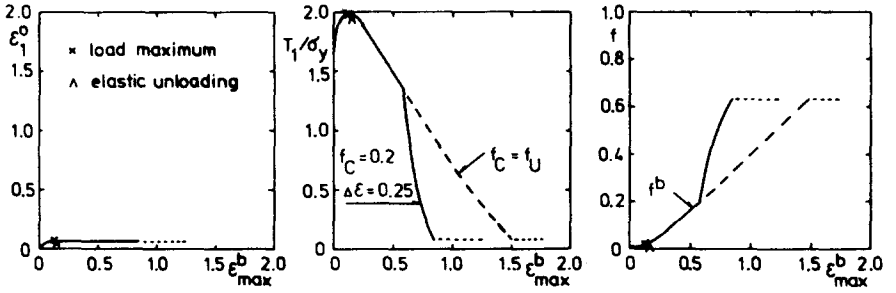

Fig. 7. Strain outside band ϵ_1^0, nominal traction T_1 and void volume fraction f, versus maximum principal logarithmic strain ϵ^b_{max} inside band; for $\epsilon_3^0 = 0$, $\sigma_2^0 = 0.25\ \sigma_1^0$, $\psi_I = 37.0°$, $f_I^b = 0.01$, $q_1 = 1.5$ and $f^*_U/f_U = 0.95$.

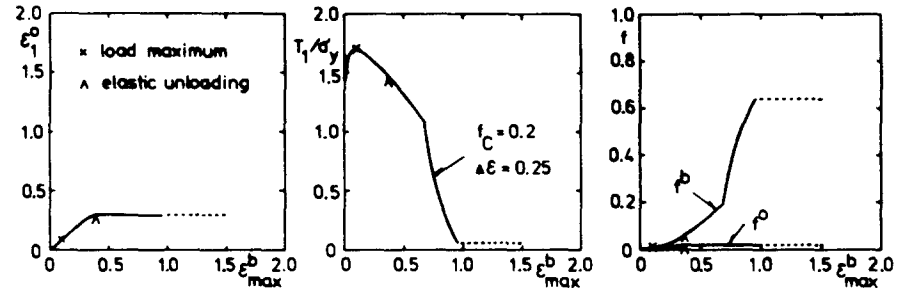

Fig. 8. Strain outside band ϵ_1^0, nominal traction T_1, and void volume fraction f, versus maximum principal logarithmic strain ϵ^b_{max} inside band; for $\epsilon_3^0 = \epsilon_2^0$, $\sigma_3^0 = \sigma_2^0 = 0.25\ \sigma_1^0$, $\psi_I = 25.0°$, $f_I^b = 0.01$, $q_1 = 1.5$ and $f^*_U/f_U = 0.95$.

which final failure occurs for the three different sets of parameters differ rather little, but are much smaller than the failure strain found using Gurson's model without the additional failure term (2.7), by specifying $f_C = f_U$.

In the case of uniaxial tension, Fig. 6, a smaller value of the strain ϵ_1^0 at localization is found for $f_C = 0.15$ and $\Delta\epsilon = 0.4$ than for $f_C = 0.20$ and $\Delta\epsilon = 0.25$. This difference occurs because for the former set of parameters the void volume fraction f_C is reached inside the band before elastic unloading takes place outside the band.

The curves shown in Figs. 7 and 8 are obtained for $\kappa = 0.25$ in (4.4), so that the stress states outside the band may be considered representative of the situations in a notched plane strain specimen and in a notched axisymmetric specimen, respectively. The results are similar with those found in the previous four figures. An additional computation for $(\dot{f})_{failure} \equiv 0$ in Fig. 7 ($f_C = f_U$) shows that, as in Fig. 5, the value of the strain ϵ^b_{max}, at which the material separates completely, is strongly influenced by using the model (2.7) to describe accelerated material failure at the later stages of void growth due to necking of the ligaments.

The computations for the simple shear band model in Figs. 3–8 illustrate various consequences of using the material failure model (2.7) and of using a fictitious final void volume fraction f^*_U slightly below the ultimate value f_U. In the linear incremental method used to obtain these solutions the size of the strain increment allowable from the point of view of numerical stability depends on the choice of the parameters $\Delta\epsilon$ and f^*_U/f_U. For material points in the range $f_C < f < f^*_U$ smaller strain increments are required, if $\Delta\epsilon$ is chosen smaller, and in the range $f = f^*_U$ the allowable strain increment decreases, if the parameter f^*_U/f_U is chosen closer to unity.

5. LOCALIZATION BETWEEN LARGER VOIDS

In a recent investigation of a ductile fracture mechanism involving the interaction of relatively large microscopic voids with small-scale voids the approximate constitutive equations for a ductile, porous medium have been used to model the smaller voids [10]. The material is taken to initially contain a periodic array of circular cylindrical voids (Fig. 9), which makes it

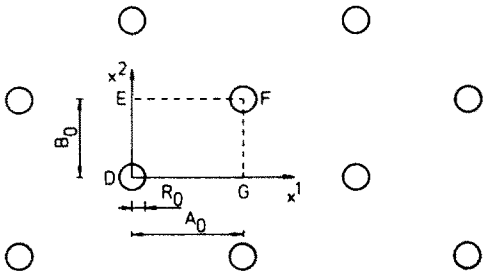

Fig. 9. Periodic array of circular cylindrical voids.

possible to reduce the computational problem by applying a number of symmetries. In the matrix material between the larger voids the volume fraction f of small-scale voids is taken to be zero initially, but nucleation occurs according to (2.5) and (2.9) or (2.10).

In this material failure of the ligament between two larger voids occurs by the formation of a shear band, in which narrow regions with high volume concentrations of small-scale voids grow from the surfaces of the larger voids. The failure criteria used in [10] are $f > 0.1$ or $f > 0.2$ over either 35, 60 and 100% of the ligament separating two larger voids. Such points of failure have been computed under plane strain conditions for various prescribed ratios of the principal stresses in the x^1- and x^2-direction and under various conditions of generalized plane strain chosen to approximately simulate material behaviour inside a round tensile bar. It is found that all these failure points for different stress states are reasonably well approximated by a single curve in a plot of the stress triaxiality parameter (mean stress/effective Mises stress) versus effective strain. This result agrees very well with recent experimental results of Hancock and Brown [21], who found a similar common fracture curve for round notched specimens and for plane strain notched specimens made of structural steels. It should be noted that such a common fracture curve is not predicted by the simpler model considered in Section 4. According to the simpler model materials are far more resistant to shear band formation when strained under axisymmetric conditions than under plane strain conditions.

Here the model of final material failure (2.7) shall be introduced in the numerical analysis of the ductile fracture mechanism involving two size-scales of voids, instead of the failure criteria used in [10]. It is not expected that this will significantly change the failure strains found in the previous analysis; but the more realistic description of the loss of load carrying capacity in the heavily damaged regions will accelerate the stress redistribution and thus better represent the growing failure process.

A detailed description of the numerical procedure has been given in [10] and shall not be repeated here. Due to symmetries only half of the region DEFG in Fig. 9 needs be analysed numerically. The grid employed in the incremental finite element solution (see Fig. 10) consists of quadrilaterals, each build up of four linear displacement triangular elements.

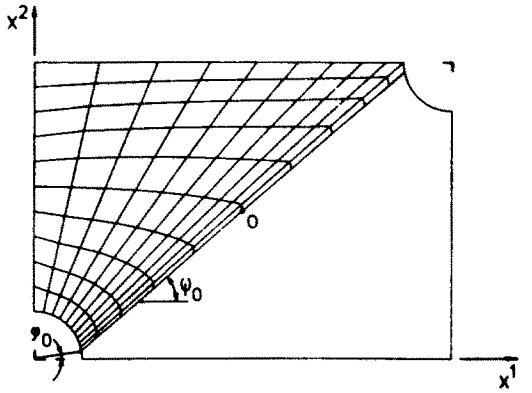

Fig. 10. Mesh used in numerical solution.

The case considered here is uniaxial plane strain tension in the x^2-direction, with the initial geometry specified by $B_0/A_0 = 0.7111$, $R_0/A_0 = 0.1167$ and $\phi_0 = 11.25°$. Thus, the initial angle of the line along which a narrow shear band can be described by the mesh is $\psi_0 = 40.8°$. The matrix material is specified by the same parameters used in Figs. 5–8, with $\sigma_y/E = 0.0033$, $\nu = 0.3$, $n = 10$, $q_1 = 1.5$ the initial void volume fraction $f_I = 0$ and plastic strain controlled nucleation $f_N = 0.04$, $\epsilon_N = 0.3$ and $s = 0.1$. Furthermore, in the material failure model (2.8) the parameter values $f_C = 0.15$ and $\Delta\epsilon = 0.6$ are used, and at "total failure" $f_f^*/f_U = 0.9$ is employed. Various sets of the parameters f_C and $\Delta\epsilon$ could give approximately equal descriptions of final material failure; but here a relatively large value of $\Delta\epsilon$ is chosen in order to increase the stable step-size in the incremental solution, and for the same reason the value f_f^*/f_U is chosen well below unity.

The average nominal traction T_{II} versus the average principal logarithmic strain ϵ_{II} in the x^2-direction is shown in Fig. 11 and compared with the result obtained in [10] for the same case without the model of final material failure ($f_C = f_U$). At an early stage of the deformation history strain concentrations develop near the cylindrical void surfaces and small-scale voids nucleate in these regions. Subsequently, the straining and the nucleation and growth of voids starts to localize in narrow bands that grow into the material from the surfaces of the larger voids at inclinations of about 40°. During this process the maximum load is reached and immediately after, the void volume fraction reaches the value f_C in one integration point, so that the failure model (2.7) and (2.8) becomes active. Figure 11 shows that subsequently, as the material separates by a void-sheet mechanism inside the growing shear band, the load decays more rapidly as a function of strain than was found in [10] for $(\dot{f})_{\text{failure}} \equiv 0$.

The first totally damaged material point ($f = f_f^*$) occurs at $\epsilon_{II} = 0.044$, and subsequently the fractured region grows until the void volume fraction equals f_f^* in a slice of material all through the ligament, at a strain ϵ_{II} around 0.075. At on intermediate stage, $\epsilon_{II} = 0.065$, the deformed grid is shown in Fig. 12 and the distribution of void volume fractions f and maximum principal logarithmic strains ϵ are shown in Fig. 13. The strain localization is most clearly

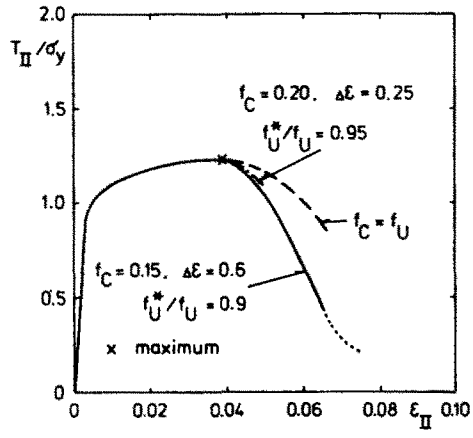

Fig. 11. Average nominal traction versus average logarithmic strain for material defined by $B_0/A_0 = 0.7111$ and $R_0/A_0 = 0.1167$, subject to uniaxial plane strain tension.

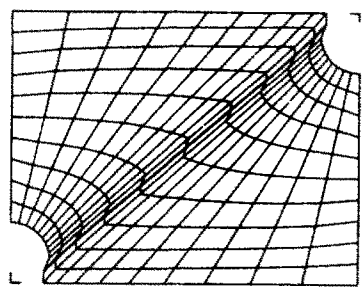

Fig. 12. Deformed grid at $\epsilon_{II} = 0.065$, for $f_C = 0.15$, $\Delta\epsilon = 0.6$ and $f_f^*/f_U = 0.9$.

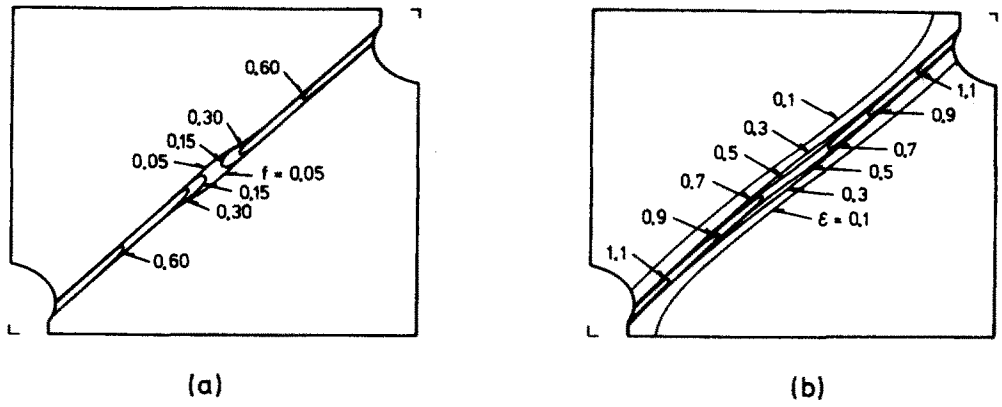

Fig. 13. Curves of constant void volume fraction f and of constant maximum principal logarithmic strain ϵ, at $\epsilon_{II} = 0.065$, for $f_C = 0.15$, $\Delta\epsilon = 0.6$ and $f_U^*/f_U = 0.9$.

illustrated by Fig. 13(b), but is also directly visible in the deformed mesh (compare Figs. 12 and 10). Figure 13(a) shows that about 45% of the ligament between the two larger voids is "totally fractured" ($f = f_U^*$) at this stage, and that the remaining part of the ligament is heavily damaged.

At the last stage of the traction versus strain curve in Fig. 11 an increasing part of the load is carried by the fictitious low stresses, due to choosing the value f_U^* smaller than f_U, in the regions where voids have coalesced. Obviously, a better approximation would be found by choosing f_U^*/f_U closer to unity; but, at the same time, smaller increments would be required for numerical stability. The gradual decay of the negative slope at the end of the curve in Fig. 11 is partly due to the chosen value of f_U^*, analogous with the final, dotted horizontal curves in Figs. 3–8, but depends also on the mesh design (Fig. 11), which enforces a doubled band width near point 0.

In Fig. 11 the initial part of the solution for failure parameters $f_C = 0.20$, $\Delta\epsilon = 0.25$ and $f_U^*/f_U = 0.95$ is shown. Naturally, with the larger value of f_C failure starts slightly later; but otherwise the curve obtained for these parameters is approximately parallel with the initial part of the curve obtained for the first set of parameters, as would be expected from the comparisons in Fig. 5. Due to the smaller value of $\Delta\epsilon$ and the larger value of f_U^*/f_U, considerably smaller increments must be used in the linear incremental solution, and thus a complete numerical solution for this set of parameters would be a great deal more costly than that obtained for the first set of parameters.

The initial volume fraction of larger voids in the present computations is 0.03; but it should be noted that in using the failure criterion based on a certain critical void volume fraction f_C, the volume fraction of larger voids is not taken into account. Naturally, the critical volume fraction represents a local measure of the size of approximately identical neighbouring voids relative to their spacing. In fact, it was emphasized by Brown and Embury[7] that in technological materials the effect of small strengthening particles and macroscopic inclusions cannot be added in defining the critical volume fraction.

6. DISCUSSION

The model applied in the present paper to describe the average macroscopic effect of final material failure by coalescence of voids is arbitrary in some respects. Introducing the extra term $(\dot{f})_{\text{failure}}$ in (2.1) means that in the later stages of deformation f is no longer just the volume fraction of holes, but a more general measure of damage, including also the concept of a volume fraction of inactive material. Furthermore, the particular functional dependencies used in (2.7) and (2.8) are by no means the only natural choices that could have been made. However, it seems that the model used does give a reasonable description of the most important effect, which is the rapid decay of material stress carrying capacity once the final process of coalescence is taking place. It should be possible in many cases to choose the values of the parameters f_C and $\Delta\epsilon$ so that observed material behaviour is reasonably well described.

The values of the critical void volume fraction f_C used here are based on experimental results[7, 8], and the nonzero values of $\Delta\epsilon$ account for small amounts of straining during

necking of ligaments and for the expectation that not all neighbouring voids coalesce simultaneously. From a theoretical point of view a more detailed understanding of the parameter values to be used in the failure model (2.8) could be obtained by numerical studies for various periodic void distributions, analogous with[4, 16, 17]. These previous numerical studies did not emphasize the development of current void volume fractions, needed to estimate f_C. However, since deformed void shapes tend to vary considerably with the degree of triaxiality of the stress state[3] some stress state dependence of f_C could be expected.

The isotropic material behaviour assumed in the Gurson model is expected to give a reasonable approximation for low void volume fractions (see [16, 17]), provided that the initial inclusion distribution is not too anisotropic. However, the final coalescence process may be highly anisotropic, and retaining isotropy of the constitutive law in this range is mainly a question of convenience in describing the rapid local decay in stress-carrying capacity.

The process of a growing failure region inside a thin slice of material analysed in Section 5 is analogous with other processes in the area of fracture mechanics that also require a complex continuum solution. The problem in Section 5 is characterized by a growing shear band inside which the material fails gradually by a void sheet mechanism; but in fact the situation shown in Fig. 13 looks much like that of a growing crack. In crack growth computations based on J_2 flow theory[22, 23] the crack extension has been modeled directly as a growing free surface, and comparison with experimental results [23] have indicated that a critical value of the crack opening angle may be a useful growth criterion after a small amount of initial extension. If the constitutive relations for a void containing material were used in such a computation, the loss of material stress carrying capacity would be the natural crack growth cirtiterion. The computation would be quite similar with that described in Section 5, and nodes could be released to extend the crack each time the ultimate void volume fraction f_U is reached at the crack tip.

It should be emphasized that the use of a fictitious elastic–plastic model to describe totally fractured material, for a fixed void volume fraction f_U^* slightly smaller than f_U, is completely independent of whether or not the material failure model (2.7) and (2.8) is included in the analysis. No material point can be allowed to exceed the ultimate value f_U of the void volume fraction, and some measure to prevent this event must be included in the analysis. Releasing nodes to create new free surfaces inside the material as fracture occurs would provide a more precise description of the failure process, and this is not too difficult in cases where the location of the nodes to be released is known before starting the computation. Letting the elements vanish when the void volume fraction reaches the value f_U^* is another possibility that is being investigated currently. This alternative description of the totally fractured material has the same advantage as the fictititous elastic–plastic model used here that a need to specify changing boundary conditions during a computation is avoided, and results obtained by the two methods are in good agreement.

From the point of view of numerical stability the fictitious elastic–plastic description of the failed zone does require small increments. However, for the values of the parameters f_U^*/f_U and $\Delta\epsilon$ used in the present investigation, the limitations on the increment size due to the failure description (2.8) are of the same order of magnitude as that resulting from the description of the failed zone.

REFERENCES

1. F. A. McClintock, A criterion for ductile fracture by the growth of holes. *J. Appl. Mech.* **35**, 363–371 (1968).
2. J. R. Rice and D. M. Tracey, On the ductile enlargement of voids in triaxial stress fields. *J. Mech. Phys. Solids* **17**, 201–217 (1969).
3. B. Budiansky, J. W. Hutchinson and S. Slutsky, Void growth and collapse in viscous solids. *Mechanics of Solids*, The Rodney Hill 60th Anniversary Volume (Edited by H. G. Hopkins and M. J. Sewell). Pergamon Press, Oxford (1981).
4. A. Needleman, Void growth in an elastic–plastic medium. *J. Appl. Mech.* **39**, 964–970 (1972).
5. A. L. Gurson, Continuum theory of ductile rupture by void nucleation and growth—I. Yield criteria and flow rules for porous ductile media. *J. Engng Materials Technol.* **99**, 2–15 (1977).
6. A. L. Gurson, Porous rigid-plastic materials containing rigid inclusions—yield function, plastic potential, and void nucleation. *Proc. Int. Conf. Fracture* (Edited by D. M. R. Taplin) **2A**, pp. 357–364. Pergamon Press, Oxford (1977).
7. L. M. Brown and J. D. Embury, The initiation and growth of voids at second phase particles. *Proc. 3rd. Int. Conf. on Strength of Metals and Alloys.*, Inst. of Metals, pp. 164–169, London (1973).
8. S. H. Goods and L. M. Brown, The nucleation of cavities by plastic deformation. *Acta Metallurgica* **27**, 1–15 (1979).
9. C.-C. Chu and A. Needleman, Void nucleation effects in biaxially stretched sheets. MRL E118, Division of Engineering, Brown University (1979).

10. V. Tvergaard, Ductile fracture by cavity nucleation between larger voids. Danish Center for Appl. Math. and Mech., Rep. No. 210 (1981).
11. J. W. Rudnicki and J. R. Rice, Conditions for the localization of deformation in pressure-sensitive dilatant materials. *J. Mech. Phys. Solids* **23**, 371–394 (1975).
12. Z. Mróz, On forms of constitutive laws for elastic–plastic solids. *Archiwum Mechaniki Stosowanej* **18**, 3–35 (1966).
13. S. Nemat-Nasser and A. Shokooh, On finite plastic flows of compressible materials with internal friction. *Int. J. Solids Structures* **16**, 495–514 1980).
14. A. Needleman and J. R. Rice, Limits to ductility set by plastic flow localization. Mechanics of Sheet Metal Forming (Edited by D. P. Koistinen *et al.*), pp. 237–267, Plenum Press, New York (1978).
15. J. F W. Bishop and R. Hill, A theory of the plastic distortion of a polycrystalline aggregate under combined stresses. *Philosoph. Mag.* **42**, 414–427 (1951).
16. V. Tvergaard, Influence of voids on shear band instabilities under plane strain conditions. *Int. J. Fracture* **17**, 389–407 (1981).
17. V. Tvergaard, On localization in ductile materials containing spherical voids. Danish Center for Appl. Math. and Mech., Rep. No. 181 (1980).
18. H. Yamamoto, Conditions for shear localization in the ductile fracture of void-containing materials. *Int. J. Fracture* **14**, 347–365 (1978).
19. M. Saje, J. Pan and A. Needleman, Void nucleation effects on shear localization in porous plastic solids. Div. of Engineering, Brown University, Rep. NSF-ENG76-16421/7 (1980).
20. J. W. Hutchinson and V. Tvergaard, Shear band formation in plane strain. *Int. J. Solids Structures* **17**, 451–470 (1981).
21. J. W. Hancock and D. K. Brown, On the role of strain and stress state in ductile failure. Dept. of Mechanical Engineering, University of Glasgow (1981).
22. H. Andersson, Finite element treatment of a uniformly moving elastic–plastic crack tip. *J. Mech. Phys. Solids* **22**, 285–308 (1974).
23. C. F. Shih, H. G. deLorenzi and W. R. Andrews, Studies on crack initiation and stable crack growth. *ASTM STP* **668**, 65–120 (1979).